NASA CR-159814



NASA

# PLASMA PHYSICS ANALYSIS OF SERT II OPERATION

Prepared for

LEWIS RESEARCH CENTER

NATIONAL AERONAUTICS AND SPACE ADMINISTRATION

GRANT NSG 3011



January 1980

Harold R. Kaufman
Department of Mechanical Engineering
Colorado State University
Fort Collins, Colorado

| 1. Report No. | 2. Government Accession No. | 3. Recipient's Catalog No. |
|---|---|---|
| NASA CR-159814 | | |

| 4. Title and Subtitle | 5. Report Date |
|---|---|
| PLASMA PHYSICS ANALYSIS OF SERT II OPERATION | January 1980 |
| | 6. Performing Organization Code |

| 7. Author(s) | 8. Performing Organization Report No. |
|---|---|
| Harold R. Kaufman | |
| | 10. Work Unit No. |

| 9. Performing Organization Name and Address | 11. Contract or Grant No. |
|---|---|
| Department of Mechanical Engineering<br>Colorado State University<br>Fort Collins, Colorado 80523 | NSG-3011 |
| | 13. Type of Report and Period Covered |
| 12. Sponsoring Agency Name and Address | Contractor Report |
| National Aeronautics and Space Administration<br>Washington, D.C. 20546 | 14. Sponsoring Agency Code |

15. Supplementary Notes

Contr. Manager, William R. Kerslake, NASA Lewis Research Center, Cleveland, Ohio 44135

This report is a reproduction of an analysis made in January 1980, and is of interest to NSG-3011.

16. Abstract

An analysis of the major plasma processes involved in the SERT-II experiments was conducted to aid in the interpretation of recent data. It is also hoped that this analysis might suggest further experiments that could be conducted with the SERT-II spacecraft.

Axially symmetric models were found to be inadequate for neutralization electron conduction to the ion beam. A plume penetration model was developed for this conduction problem, and showed qualitative agreement with flight data. In the absence of data to the contrary, this plume penetration model is recommended for future calculations.

In the SERT-II configuration, conduction of neutralization electrons between thrusters was experimentally demonstrated in space. The analysis of this configuration presented herein suggests that the relative orientation of the two magnetic fields was an important factor in the observed results. Specifically, the opposed field orientation appeared to provide a high conductivity channel between thrusters, and a barrier to the ambient low-energy electrons in space.

The SERT II neutralizer currents with negative neutralizer biases were up to about twice the theoretical prediction for electron collection by the ground screen. An explanation for the higher experimental values was a possible conductive path from the neutralizer plume to a nearby part of the ground screen.

Plasma probe measurements on SERT II gave the clearest indication of plasma electron temperature, with normal operation being near 5 eV and discharge only operation near 2 eV.

| 17. Key Words (Suggested by Author(s)) | 18. Distribution Statement |
|---|---|
| Plasma Physics<br>Neutralization<br>Ion Sources | Unclassified-Unlimited<br>N80-27189# |

| 19. Security Classif. (of this report) | 20. Security Classif. (of this page) | 21. No. of Pages | 22. Price* |
|---|---|---|---|
| Unclassified | Unclassified | | |

* For sale by the National Technical Information Service, Springfield, Virginia 22161

TABLE OF CONTENTS

# INTRODUCTION

Recent SERT-II tests have included a number of experiments that were not included in the original program plans.[1,2] Of particular interest are those experiments involving interactions between the two thrusters. Being the only such experiments in a space environment, these experiments have been a valuable extension of the original program.

An analysis of the major plasma processes involved in the SERT-II experiments was felt to be an important aid in the interpretation of the recent data. This analysis is presented herein. It is also hoped that this analysis might suggest further experiments that could be conducted with the SERT-II spacecraft, thereby providing additional information about the operation of electric thrusters in space.

Because of the complexity of the plasma distribution around a spacecraft, simplifying assumptions are desirable. Foremost of the assumptions used is the somewhat arbitrary division of the analysis into separate parts. Following the analysis of these different problem parts, the results are assembled to simulate operation in different modes. This simulated operation is then compared to data from flight experiments.

Some of the more frequently used plasma calculations are described in Appendix A. The calculation procedure for a charge-exchange plasma is presented in Appendix B. The calculation procedure developed for the neutralizer plume region is included in Appendix C. All equations are in SI (mks) units unless stated otherwise. An exception to SI units is the electron temperature. Unless otherwise noted, this temperature is in electron volts (eV).

It should be kept in mind that plasma calculations are more approximate than most other scientific calculations, often being uncertain to a factor of two. The presence of two or three significant figures in some calculations results from a desire to avoid additional error due to round-off, and does not necessarily indicate the inherent accuracy of the calculation.

## PROBLEM DEFINITION

The overall problem was divided into the following parts:

1. The overlap region of conducting plasmas downstream of both thrusters.
2. The ion beam generated by each thruster.
3. The charge-exchange plasma between a neutralizer and an ion beam.
4. The coupling characteristics of the neutralizers.
5. The collection of electron current by the ground screen surrounding a thruster.
6. The collection of charge-exchange ion current from one thruster by the accelerator grid of the other thruster.
7. The collection of electron current by the spacecraft.

A variety of operating conditions was considered, as appropriate, for each of the above problem parts. These conditions included:

1. Normal operation. With high voltages on (+3000 V and -1500 V), an 85 mA Hg ion beam, and a total propellant flow rate of 142 mA-equiv.

2. Discharge only. With accelerator grid grounded and a low energy ($\sim$ 40 eV) 80 mA beam of Hg ions generated. Total propellant flow rate is again about 142 mA-equiv. The neutralizer is operational, but this mode permits some electrons to escape from the discharge chamber, so that few electrons are required from the neutralizer.

3. Neutralizer only. The neutralizer is operational, but no beam of any kind is generated by the discharge chamber.

4. Thruster off (non-operating). No neutralizer or discharge-chamber discharge. The accelerator may be at -1500 V.

The electron temperature has been observed in the beams and surrounding charge-exchange plasmas during various SERT-II ground tests. Two values, 2 eV and 5 eV, are felt to span the range of mean electron temperature indicated by these ground tests. Both of these values will be used for the calculations herein.

The overall spacecraft, including upper stage and solar array panels, is shown in Fig. 1. The spacecraft, as defined in SERT-II program terminology, is also shown in Fig. 2. An experimental magnetic field plot of a SERT-II thruster (backup thruster 1 E 1) was obtained as a part of this analysis and is shown in Fig. 3. A plot of the magnetic field integral $\int_o^r \bar{B} \times d\bar{r}$ was also obtained and is shown in Fig. 4. This integral was obtained by integrating radially outwards from the thruster axis, so that the integral value was defined as zero on the axis. The calculation of various currents and potential drops requires knowledge of this integral. To be completely rigorous, the integration should be in the direction of the current flow.* But the current flow of interest (normal to the magnetic field direction) is close enough to the radial direction to use Fig. 4.

The spatial relationship between the thruster, beam, and neutralizer plume is indicated in Fig. 5 for normal operation. The approximate location of the beam edge was determined from both ground tests and

---

*If the configuration had been two-dimensional instead of axisymmetric, then the lines of constant integral value would have corresponded to particular lines in the magnetic field plot. The integral values would have then been dependent only on the end points, and not the path of integration.

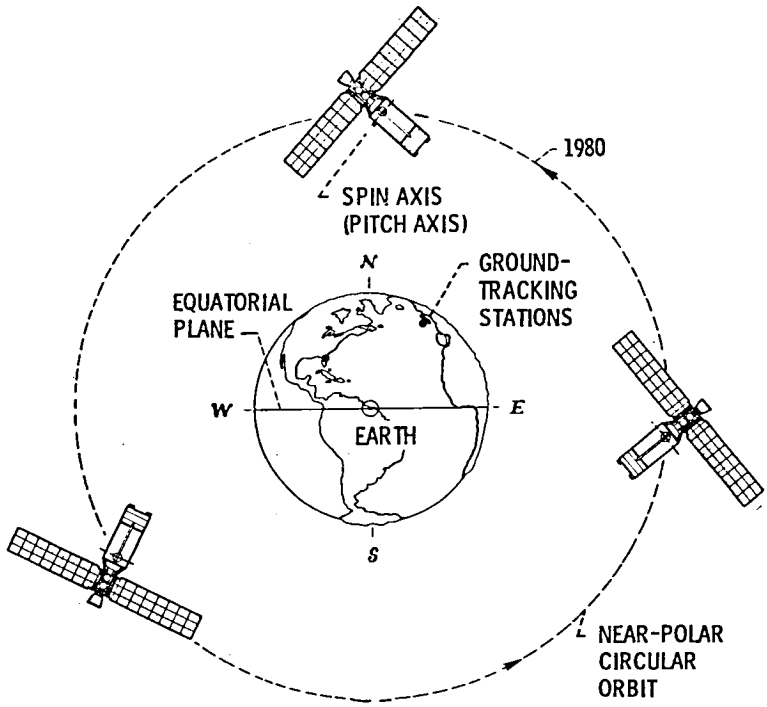


SPIN-STABILIZED POSITION

VEHICLE COORDINATE SYSTEM IN ORBIT VIEWED FROM SUN

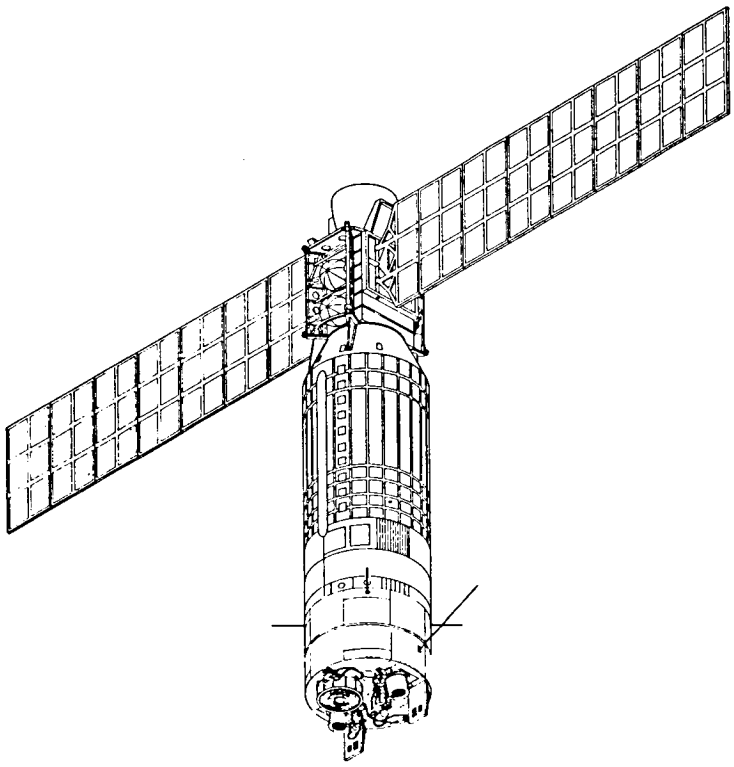

Fig. 1 - SERT-II spacecraft with upper stage and solar array panels.

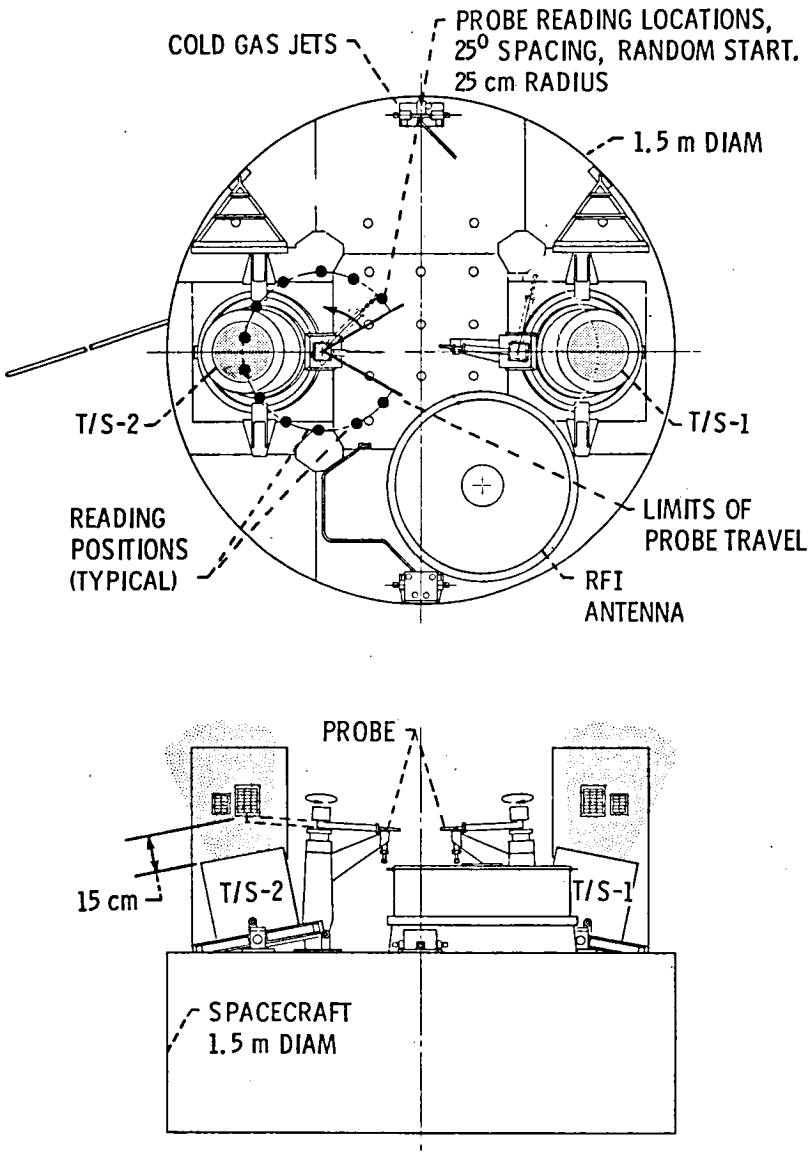


Fig. 2 - Enlarged view of SERT-II spacecraft.

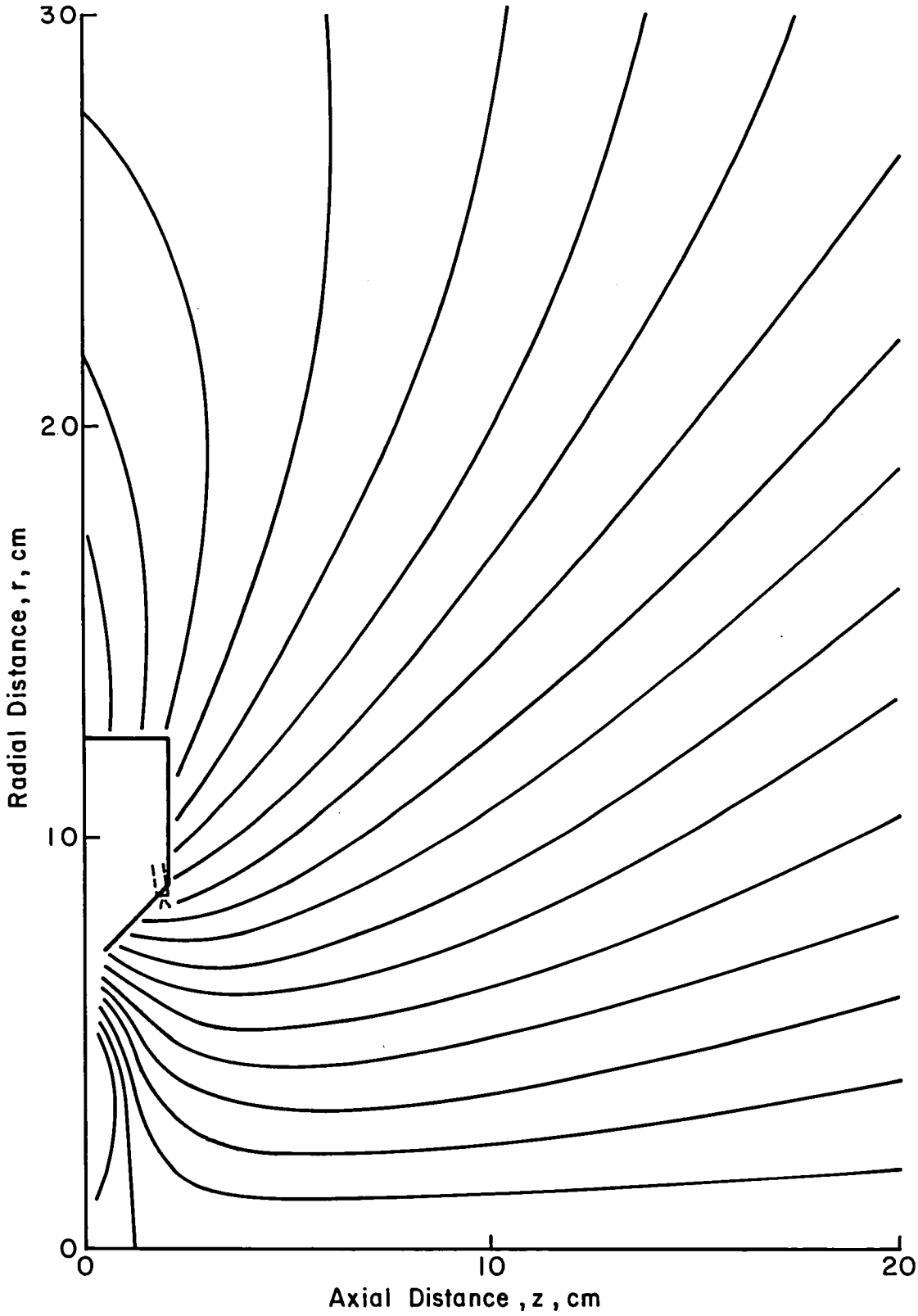


Fig. 3 - Plot of magnetic field lines downstream of thruster.

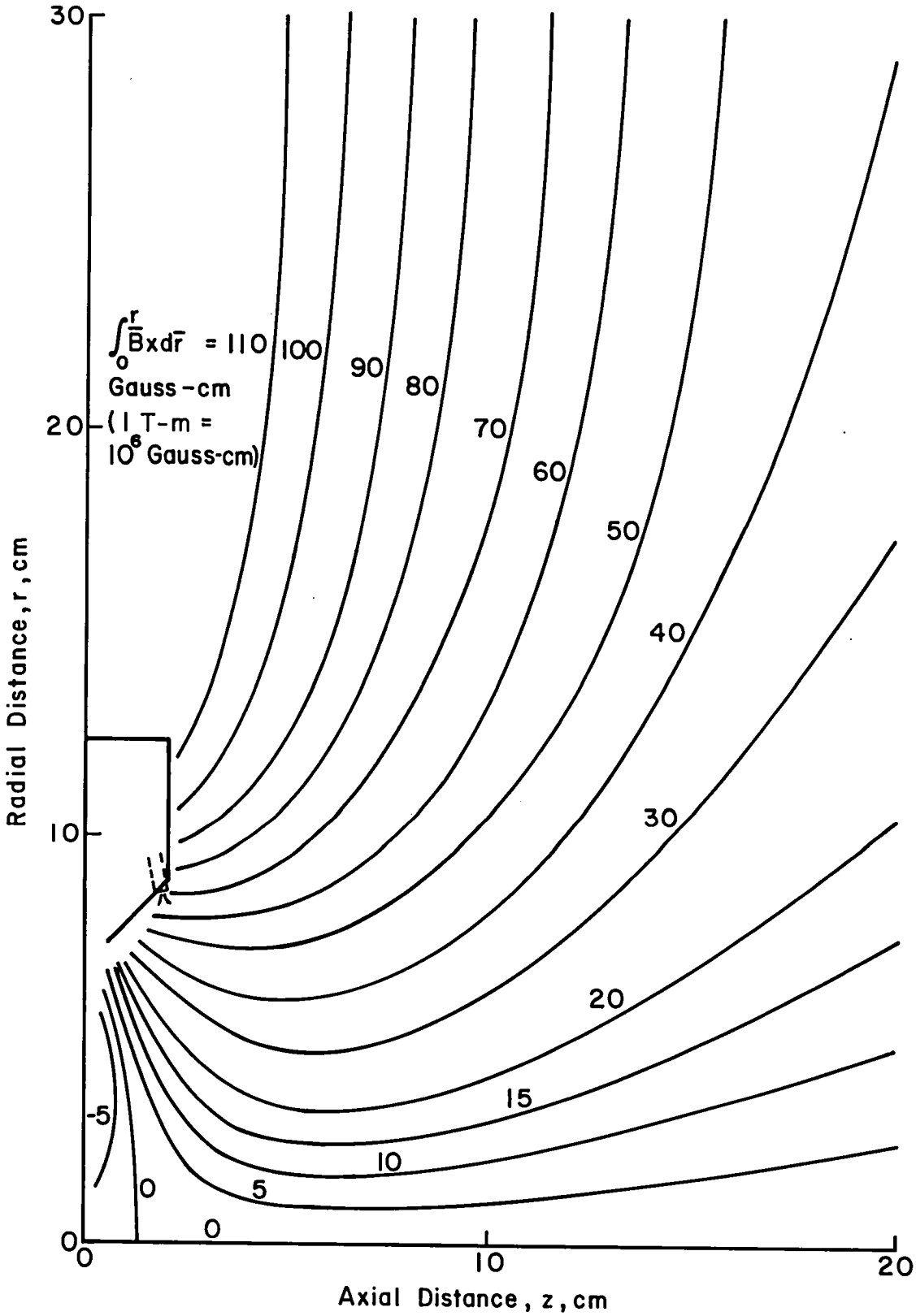


Fig. 4 - Plot of magnetic field integral values (from axis).

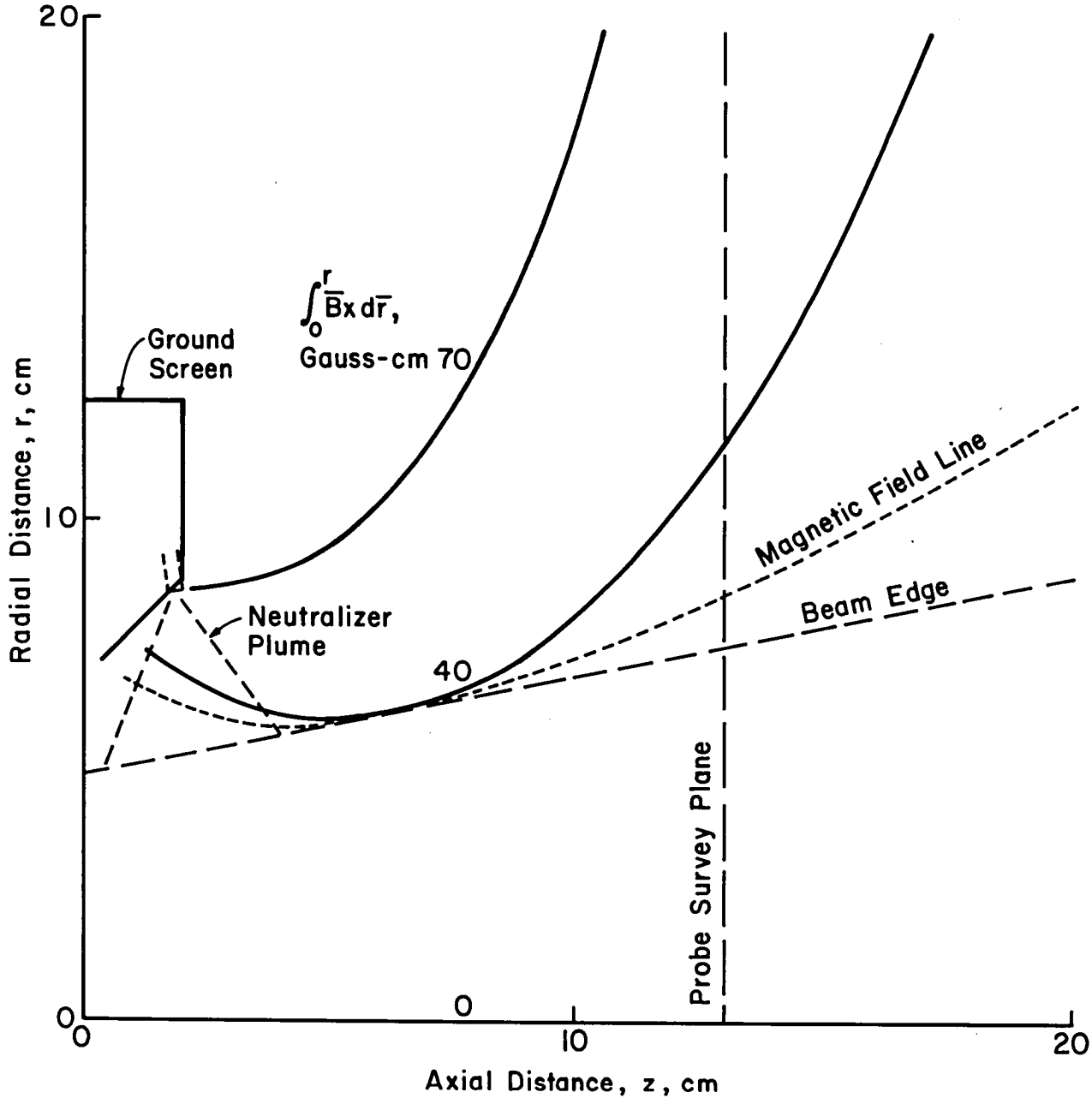


Fig. 5 - Relationship of beam, neutralizer plume, and magnetic field for normal operation.

the potential probe used in space (at the probe survey plane indicated in Fig. 5). The beam edge is actually more indefinite than indicated in Fig. 5, but the decrease in density occurs over a small enough region that the uncertainty in calculated values due to the uncertainty in effective beam edge is not large. The significance of integral and magnetic field lines shown in Fig. 5 is discussed in the Analysis section.

For discharge only operation the edge of the ion beam is shifted outwards about 1.5 cm in the probe survey plane. The beam diameter at the accelerator grid was assumed unchanged from normal operation.

The approximate overall shape of the magnetic field due to both thrusters on the spacecraft (in the absence of earth's field) is indicated in Fig. 6. For far field effects, the thrusters were found to have dipole moments of about 27 $A\text{-}m^2$. The two thrusters were mounted on the spacecraft with opposite polarities, as also indicated in Fig. 5. The dipole approximations for the thrusters were used to determine the approximate location of the field line joining the axes of the two thrusters.

The strength of earth's field at orbital altitude is roughly $3 \times 10^{-5}$ T (0.3 Gauss). Using the dipole approximation, the field of a thruster on axis (the beam direction) would equal that of earth at about 0.5 m from a thruster. The outer parts of the field distribution shown in Fig. 6 would thus change drastically as a function of the spacecraft orientation relative to earth's field.

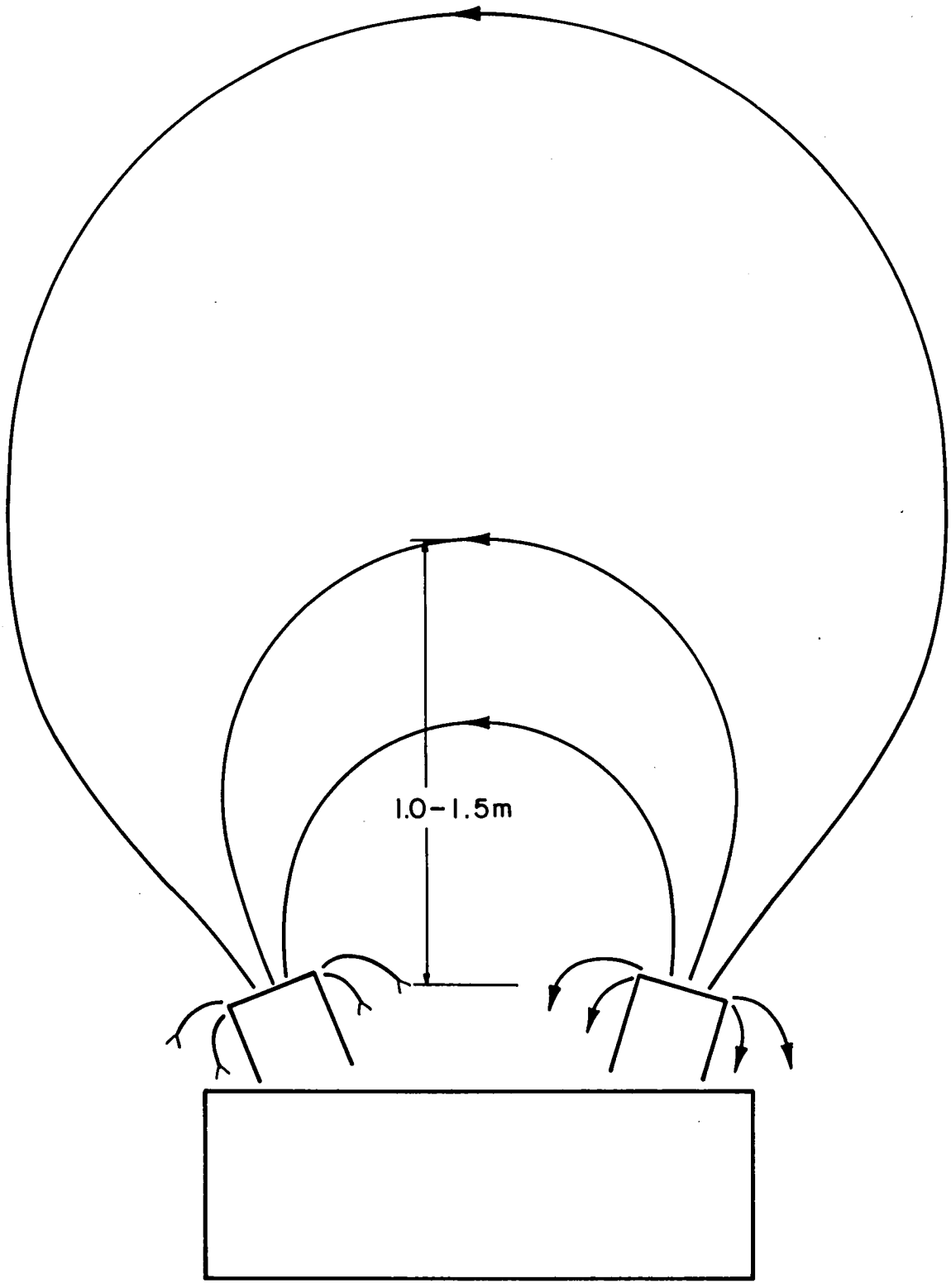


Fig. 6 - Sketch of overall magnetic field shape.

# ANALYSIS

As described in the Introduction, the analysis is initially carried out for parts of the overall problem. The first of these parts to be analyzed is the overlap region downstream of the thrusters.

## Overlap Region

The region where the effluxes from the two thrusters overlap is an important one for conduction of electrons from the vicinity of one thruster to the vicinity of the other. One might expect the effective connection between the two effluxes to be at a large distance from the spacecraft and involve ambient electrons from space. This expectation would have some justification in the absence of a significant magnetic field external to the thrusters. The relatively large potential wells formed by energetic electrons from the thrusters would readily capture the colder ($\sim$ 0.2 eV) electrons from space. This capture would result in a reduction of positive well depth, the escape of the more energetic electrons, and an eventual electron temperature near the thrusters that is close to that of ambient space.

The thrusters do, however, produce a significant magnetic field in the region surrounding the thrusters. Although there is considerable distortion of this field due to interaction with earth's magnetic field (discussed in connection with Fig. 6), there are far fewer field lines to cross in going from one thruster to another than in going from either thruster to space far from that thruster. For example, there is a region slightly downstream of the thrusters where the field due to the thrusters is either negligible or parallel to the conduction path between thrusters. The magnetic field of earth would cause distortion in this region, but the cyclotron radius for a 2-5 eV electron in a

$0.3 \times 10^{-6}$ T field is about 0.2 m, so that earth's field should not be much of an obstacle for this short conduction path length close to the thrusters.

The preferred path for an electron current between thrusters thus appears to be close to the thrusters, through the charge-exchange plasma. Ignoring the small field in this region, the conductivity is given by Eq. (A-4), $\sim$ 3-10 $\times 10^3$ mhos/m for a 2-5 eV electron temperature. Plasma conductivity is clearly not a restriction.

Next, the current capacity of this region should be considered. This capacity requires an estimate of plasma density. The location for which the estimate was made was 0.2 m downstream of the thrusters. The radial distance from each of the thrusters at this location was about 0.6 m. Using the procedure of Appendix B, a normally operating thruster should produce a plasma density of about 6-4 $\times 10^{11}$ $m^{-3}$. (The first number is again for a 2 eV electron temperature, while the second is for 5 eV.) A thruster in the discharge only mode should generate a density of about 12-7 $\times 10^{11}$ $m^{-3}$. Using Eq. (A-2), the current density at the two-stream instability limit for one normally operating thruster and one discharge only thruster (plasma density of 18-11 $\times 10^{11}$ $m^{-3}$) should be about 0.22 $A/m^2$.* The cross sectional area for the current path in this overlap region need only be about 0.4 $m^2$ for the current capacity to be adequate for conducting neutralization levels of currents (85 mA) between thrusters. This current capacity,

---

*Note that the higher velocity of the 5 eV electrons is offset by the lower plasma density, resulting in the same saturation current density for both electron temperatures.

together with the high conductivity given earlier indicates that the path selected is the one that probably accounts for the bulk of actual conduction.

For the case of one normally operating thruster and one with neutralizer only, the charge exchange plasma in the overlap region would be reduced to essentially the density from the normally operating thruster alone. This would be a reduction in density by approximately a factor of three. With current capacity proportional to plasma density, the current capacity would also be reduced by a factor of about three. Although this is less than the value found above, it is still more than adequate for the few milliamperes that were observed to cross over from a neutralizer only thruster.

## Ion Beam

Another element in the circuit from one thruster to the other, or from one thruster to ambient space, is the ion beam itself. Consider first conduction in the axial direction. From Figs. 3 and 5, the ion beam roughly follows magnetic field lines, so that conduction along the beam approximates conduction parallel to the magnetic field, at least close to the thrusters. With the conductivity again $3\text{-}10 \times 10^3$ mhos/m (Eq. (A-4)), neutralizing currents will produce potential gradients of, at most, a few mV/m. Close enough to a thruster for the magnetic field and ion beam to be roughly parallel (less than about 0.5 m), the potential gradients parallel to the beam direction are thus negligible.

The current capacity parallel to the beam direction is also no obstacle to the flow of neutralization magnitude currents. For normal operation, the mean ion density close to the thruster (5 cm radius)

is $1.3 \times 10^{15}$ $m^{-3}$, while for discharge only operation the density is $1.0 \times 10^{16}$ $m^{-3}$. The corresponding current densities for the two-stream instability limit are 160-260 $A/m^2$ (2-5 eV) for normal operation and 1200-2000 $A/m^2$ for discharge only operation. For the ion beam cross section near the thruster, these current densities would give currents of 1.3-2.0 A (2-5 eV) for normal operation and 9-16 A for discharge only operation.

The beam cross sectional area increases with increasing distance from the thruster. The decrease in density, though, cancels the effect of increasing area, giving the same maximum current capacity. Thus, for the region where the beam is roughly parallel to the magnetic field, the current capacity within the ion beam far exceeds any requirement for neutralization.

Next, consider conduction in the radial direction within the ion beam. This calculation can be simplified by noting that the beam radius changes nearly linearly with beam length, and both the magnetic field strength and plasma density vary nearly inversely as the beam radius squared. With the high conductivity in the beam direction, the radial potential should independent of axial location. Putting all of this together, the radial current per unit of beam length is nearly independent of axial location.

The effective length of the ion beam where the beam and magnetic field are roughly parallel begins a few centimeters downstream of the thruster and ends 0.4 or 0.5 m from the thruster, where the earth's magnetic field will approximate the strength of field from the thruster. A value of 0.4 m was assumed for this effective length.

With the effective length assumed and the mean densities given previously, the remaining required parameter for a radial potential difference is the magnetic field integral. For the magnetic integrals shown in Fig. 4 and the beam shape shown in Fig. 5, the mean product of beam radius and magnetic integral is about $2.0 \times 10^{-6}$ T-m$^2$ for normal operation. For discharge only operation, the slightly larger beam diameter would give a mean product closer to $2.2 \times 10^{-6}$ T-m$^2$. Using these values, a neutralization current of 85 mA would give a total radial potential difference of 1.1 V for normal operation, and about 0.15 V for discharge only operation.* Thus, although the radial potential difference is much larger than the axial potential difference, it is still only a small part of observed coupling voltages ($\sim$ 30 V for normal operation).

For the current capacity in the radial direction within the ion beam, the two-stream instability limit divided by 16 should be used (see Appendix A). Using this current density and the outside area of the beam, where the current density is the greatest, current capacities in the radial direction are found to be the same as in the axial direction. That is, well above any requirement for neutralization.

---

*These voltages assumed that the full 85 mA neutralization current entered the outside of the ion beam and terminated in a uniform distribution over beam area. As mentioned in the Problem Definition section, the magnetic integrals of Fig. 4 were integrated in the radial direction. The direction normal to the magnetic field would be more precise, but this direction is not far from the radial direction used.

## Charge-Exchange Plasma Near the Thruster

The charge-exchange plasma properties are required to calculate the conduction properties of this region. Using the methods of Appendix B and a mean radius between the beam and the neutralizer, the plasma density near the thruster was found to be $5.8\text{-}3.6 \times 10^{14}$ $m^{-3}$ (2-5 eV) for normal operation and $11.5\text{-}7.3 \times 10^{14}$ $m^{-3}$ for discharge only operation. For the two-stream instability limit, the current densities are 72 and 140 $A/m^2$.

The major calculation difficulty for conduction through this charge-exchange plasma concerns the effect of the neutralizer plume. To illustrate this difficulty, first assume that the current from the neutralizer is conducted to the beam in an axially symmetric manner through the charge-exchange plasma.

Using the methods of Appendix B, a detailed distribution of plasma density was calculated. The current conducted was numerically integrated over this detailed plasma distribution. The integrated current was found to be equivalent to assuming conditions near the thruster extended 12 cm in the downstream direction. This equivalent calculation (12 cm long, constant properties) was used in all subsequent calculations. The magnetic field integral to be crossed was about $30 \times 10^{-6}$ T-m for normal operation and $25 \times 10^{-6}$ T-m for discharge only operation.

With the values given above and in Eq. (A-6), a neutralization current of 85 mA produced a potential difference of 100-160 V for normal operation and 45-71 V for discharge only operation. These values were far beyond the potentials observed, in either flight or ground tests.

For the next refinement, we note that no limitation was placed on the circulating current in the above axially symmetric calculation. With $j_{inst}$ as an upper limit, the potential difference should correspond to $j_m = j_{inst}/16$. The potential difference at 85 mA would then be 23-37 V for normal operation and 19-31 V for discharge only operation. These values are more reasonable, but will be shown to be still too high to agree with flight data.

The calculation difficulty, as indicated above, involves the neutralizer plume. In short, the plume forms a high conductivity bridge across the charge-exchange plasma. For a high current density (and plasma density) in the plume, the surrounding charge-exchange plasma can support only a portion of the circulating current density required for Eq. (A-6). The potential difference generated by the neutralizer current is therefore a lower value than would be obtained from Eq. (A-6).

Plasma conduction problems treated in the literature consider axially symmetric problems, or problems in which no circulating current is permitted to flow. The case between these two extremes is of interest for the neutralizer plume. The theoretical approach used herein for the plume is derived in Appendix C. This derivation assumes that the electron diffusion process is the same within the neutralizer plume as it is in the charge-exchange plasma. But the limitation on circulating current density serves to rotate the electric field and current density vectors within the plume, thereby facilitating conduction along the plume.

As described in Appendix C, the plume penetration mode is assumed to exist whenever that mode gives smaller local potential differences

than the axially symmetric mode. This condition is met at high current densities in the neutralizer plume. In practice, the current density starts out at a very high value at the neutralizer tip and decreases with increasing distance from the neutralizer. The plume penetration mode should thus be found close to the neutralizer and, at some sufficiently large distance, the conduction should more closely approximate the axially symmetric model.

The neutralizer plume spreads at approximately ±30 degrees. The distance from the neutralizer to the ion beam is about 3.3 cm for normal operation (see Fig. 5) and about 3.0 cm for discharge only operation. From Fig. 4, the magnetic integral is about $30 \times 10^{-6}$ T-m for normal operation and about $25 \times 10^{-6}$ T-m for discharge only operation.* Further, for a penetrating plume, the electron temperature is assumed to be about 1 eV, the plume value observed in neutralizer component tests. With these assumptions, the plume is assumed to fully penetrate the charge-exchange plasma and reach the ion beam at a neutralizer current of 10-8 mA (2-5 eV electron temperature in the surrounding charge-exchange plasma) for normal operation, and 17-13 mA for discharge only operation. The corresponding potential difference for these conditions is 4.0-5.0 V for normal operation and 3.0-3.6 V for discharge only operation. These values were obtained by integrating the potential gradient along the plume length.

---

*The magnetic integrals given here are not the mean values over the plume length. Instead, they are the smallest integral values for which a direct contact can be made through the neutralizer plume to the ion beam. The ease of conduction along magnetic field lines should assure that this lesser quantity of magnetic field will be the actual value crossed in reaching the beam through the plume.

Using the transition condition of the local potential drop being equal for Eqs. (A-6) and (C-7), the plume penetration length will vary proportionally with neutralizer current for smaller currents. The potential drop over this partial penetration length will vary as the square of the neutralizer current. For higher currents, the potential drop will vary inversely with neutralizer current. The plume might be expected to penetrate the ion beam as the neutralizer current is increased, but the high density of the ion beam would require a large increase in neutralizer current before this would happen.

The model described above for penetration of the charge-exchange plasma by the neutralizer plume is felt to be a major improvement over the alternative of assuming axial symmetry at all operating conditions. Although it is in qualitative agreement with the low impedance observed experimentally, it has not been verified with detailed probe measurements. Until such verification is obtained, calculations using this model must be assumed to have even more uncertainty than most plasma calculations.

## Neutralizer Coupling

The general problem of conduction from the neutralizer to the ion beam through the charge-exchange plasma was discussed in the preceding section. The theories presented therein are used in this section to construct neutralizer coupling models. That is, to predict the current-voltage relationships for neutralizer current conduction to the ion beam.

The axially symmetric model was described in the last section as being deficient. The axially symmetric model is also used herein to

permit the deficiency to be explored in more detail. The neutralizer coupling characteristics are shown in Fig. 7 for axially symmetric conduction, both with and without a limit on circulating current density. Except for a small radial potential drop in the ion beam (see the Ion Beam section), the variations shown in Fig. 7 are entirely the result of the potential drops in the charge-exchange plasma calculated with Eq. (A-6). It may also be noted that the current drops to zero at a total potential difference of 10 V. This is because a constant neutralizer-to-plume difference was added to the variable difference in the charge exchange plasma.

The neutralizer coupling characteristics for the plume penetration model are shown in Fig. 8. The potential differences involved in the neutralizer coupling for this model are shown in Fig. 9. The neutralizer plume is assumed to fully penetrate the charge-exchange plasma for all current values above the 8-17 mA range discussed in the previous section. At higher currents, the potential difference along the plume varies inversely with current. The radial potential difference in the ion beam is still small compared to the plume difference for discharge only operation, so the total potential difference asymptotically approaches 10 V as the current increases in Fig. 8(a). (A constant 10 V neutralizer-to-plume difference was again assumed for the plume penetration model.) For normal operation, the radial potential difference in the ion beam is larger, resulting in a minimum coupling voltage at 0.05-0.06 A.

At the lowest currents, the neutralizer does not fully penetrate to the ion beam (see Fig. 9(a)). As a result, the total potential drop must also include a term due to axially symmetric conduction. The maximum coupling voltage for each curve corresponds to the plume penetrating $\sim$ 3/4 of the charge-exchange plasma.

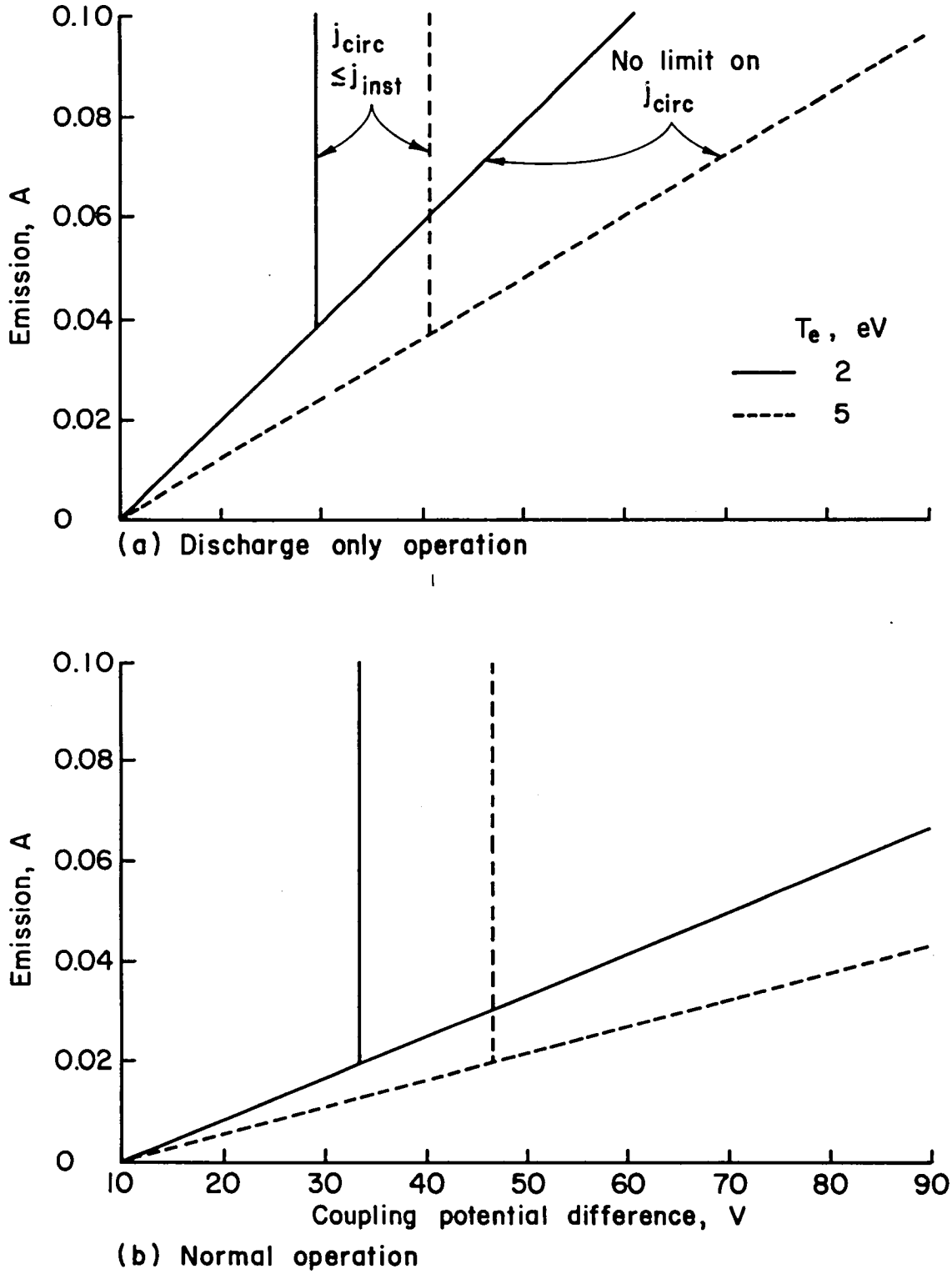


Fig. 7 - Theoretical neutralizer coupling characteristics with axially symmetric model.

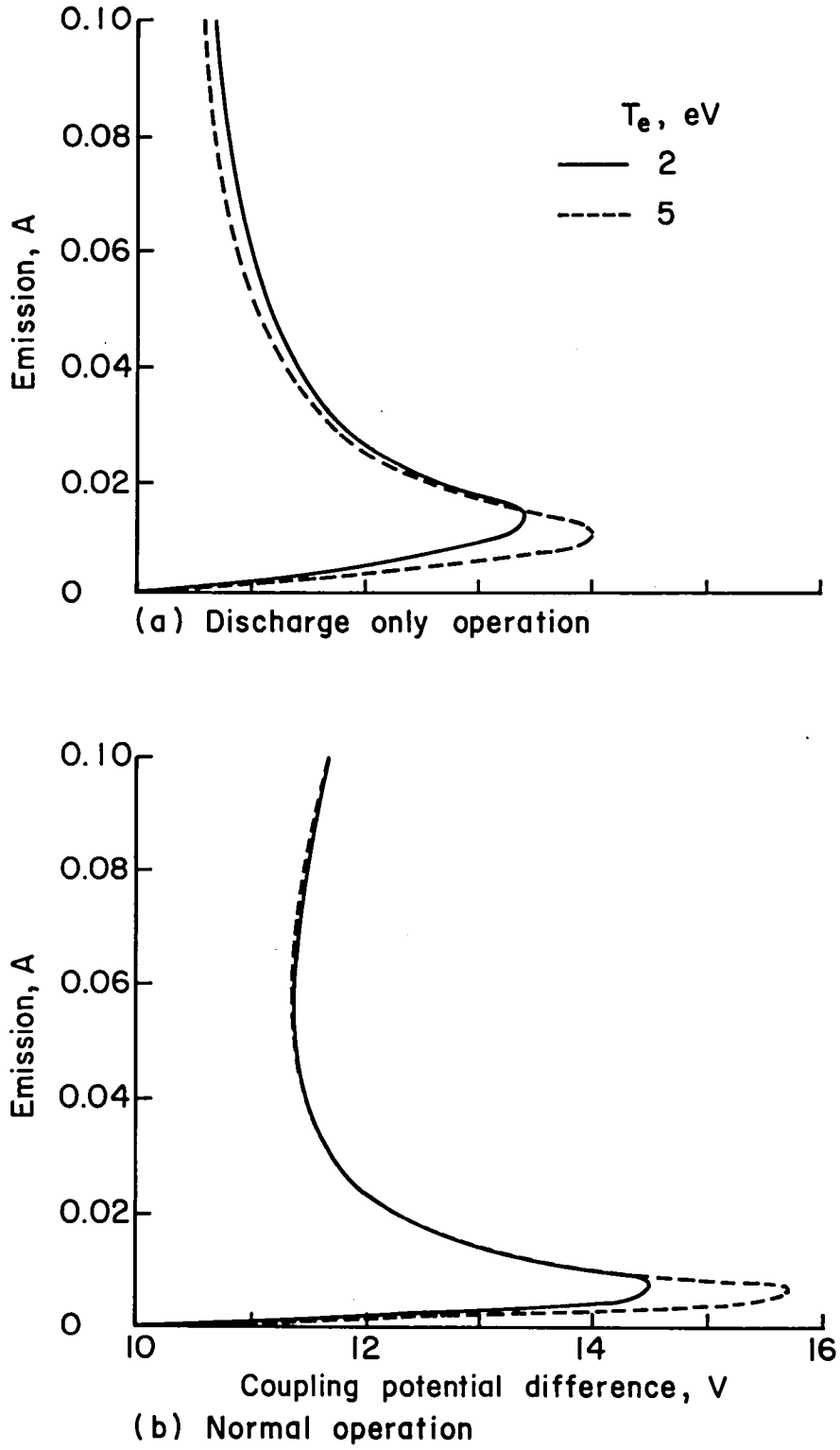


Fig. 8 - Theoretical neutralizer coupling characteristics with plume penetration model.

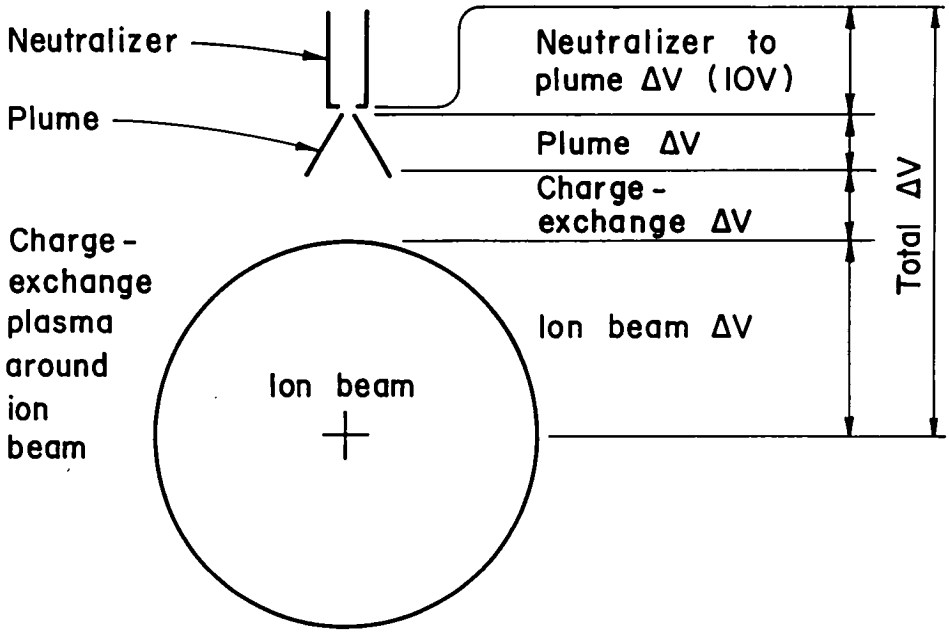


(a) Low neutralizer current with partial plume penetration

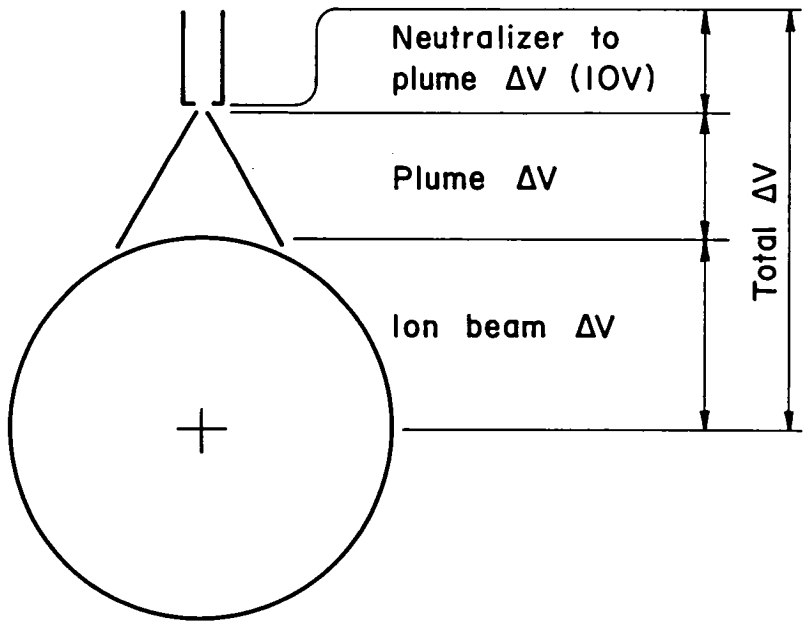


(b) High neutralizer current with complete plume penetration

Fig. 9 - Potential differences involved in neutralizer coupling with ion beam.

As will be discussed in the Comparison to Flight Data section, the plume penetration model has shortcomings when compared to flight data. At the same time, it appears to be a substantial improvement over axially symmetric models.

The neutralizer coupling characteristics presented in this section included no effect of plasma density variations on total potential difference (see discussion with Eq. (A-7)). These coupling characteristics are used in a relative manner to determine the fraction of total neutralization current expected from each of two neutralizers. Because both neutralizers will have about the same net density difference from plume to overlap region, most, or all, of the effects of density difference on potential will cancel.

### Current to Ground Screen

If the ground screen around the thruster is sufficiently positive relative to the surrounding plasma, it will draw an electron current from that plasma. The ambient plasma is due to charge exchange, so the bulk of the exposure is at the downstream face of the ground screen, where the plasma is the most dense.

Consider first operation with the neutralizer plume just penetrating the charge-exchange plasma to reach the ion beam. Referring to Fig. 5, it is seen that the magnetic field line that is tangent to the outside of the ion beam reaches approximately the inner edge of the ground screen. (This was also true of the configuration assumed for discharge only operation.) To reach a significant area of ground screen, then, the electrons must reach the ion beam through the connecting plume, be distributed circumferentially by the dense plasma in

the ion beam, then diffuse radially outwards across the magnetic field lines to obtain access to a significant area of ground screen.

The outward diffusion of electrons is associated with a potential gradient in the plasma, being most positive at the outermost diffusion radius. Over most of the ground screen involved in electron collection, then, the ground screen is more positive than the charge-exchange plasma. The collection of electrons by the ground screen is therefore assumed to be at the stability limit value. The outward diffusion is described by Eq. (A-6). From Fig. 4, the magnetic field integral to be crossed is estimated at about $25 \times 10^{-6}$ T-m per cm of ground screen involved.

There is one aspect of this calculation that should be emphasized. The model above has the neutralizer current coming radially inwards through the neutralizer plume, then radially outwards through the charge-exchange plasma. This aspect poses no serious physical problem. A dense conducting plume should be able to conduct readily, with most induced currents in the charge-exchange plasma limited to the vicinity of the plume. The majority of the charge-exchange plasma should thus be available to approximate axial symmetry in the conduction radially outwards. The problem is more one of deciding the depth of penetration for the plume. The transition from plume to axially symmetric conduction was described in Appendix B as being calculated from the relative impedance of the two alternate conduction paths. Here the alternate path is being used for conduction in the opposite direction.

For simplicity, only fully penetrating plumes are considered in this section. Also, the current required for full penetration was assumed to be the same as found earlier for neutralizer coupling to the ion beam, 10-8 mA for normal operation and 17-13 mA for discharge only operation.

The ground screen collection current is shown in Fig. 10 as a function of neutralizer bias. The total potential difference at each current was assumed to consist of three contributions. The first was the plume potential difference, which varies inversely with neutralizer current for the full-penetration condition that was assumed (Eqs. (C-7)).

The second was the radial potential difference in the charge-exchange plasma (Eq. (A-6)). This second difference was integrated radially to include the effect of varying current due to partial collection at each increment in radius. If the radial current density was large enough to generate a circulating current density above the instability limit, the local radial difference was reduced to a value consistent with $j_{circ} = j_{inst}$. As discussed in Appendix A, it appears reasonable from a physical viewpoint to assume that enhanced diffusion across magnetic field lines can result when the circulating current density reaches the instability limit. The straight-line portions of the curves in Fig. 10 correspond to this limit on circulating current density.

Because conduction was to the ground screen in Fig. 10, the third potential difference included was that due to the plasma density difference. The neutralizer plume, with an $\sim$1 eV electron temperature, has shown little variation along its length in ground tests. A similar lack of potential difference due to density difference is therefore assumed herein. In a similar manner, the low energy of plume electrons is expected to cause little or no "barometric" effect at the plume-beam boundary. The most significant density effect, and the one included, was the density difference between the ion beam and the surrounding charge-exchange plasma. Using the beam density at the plane of the

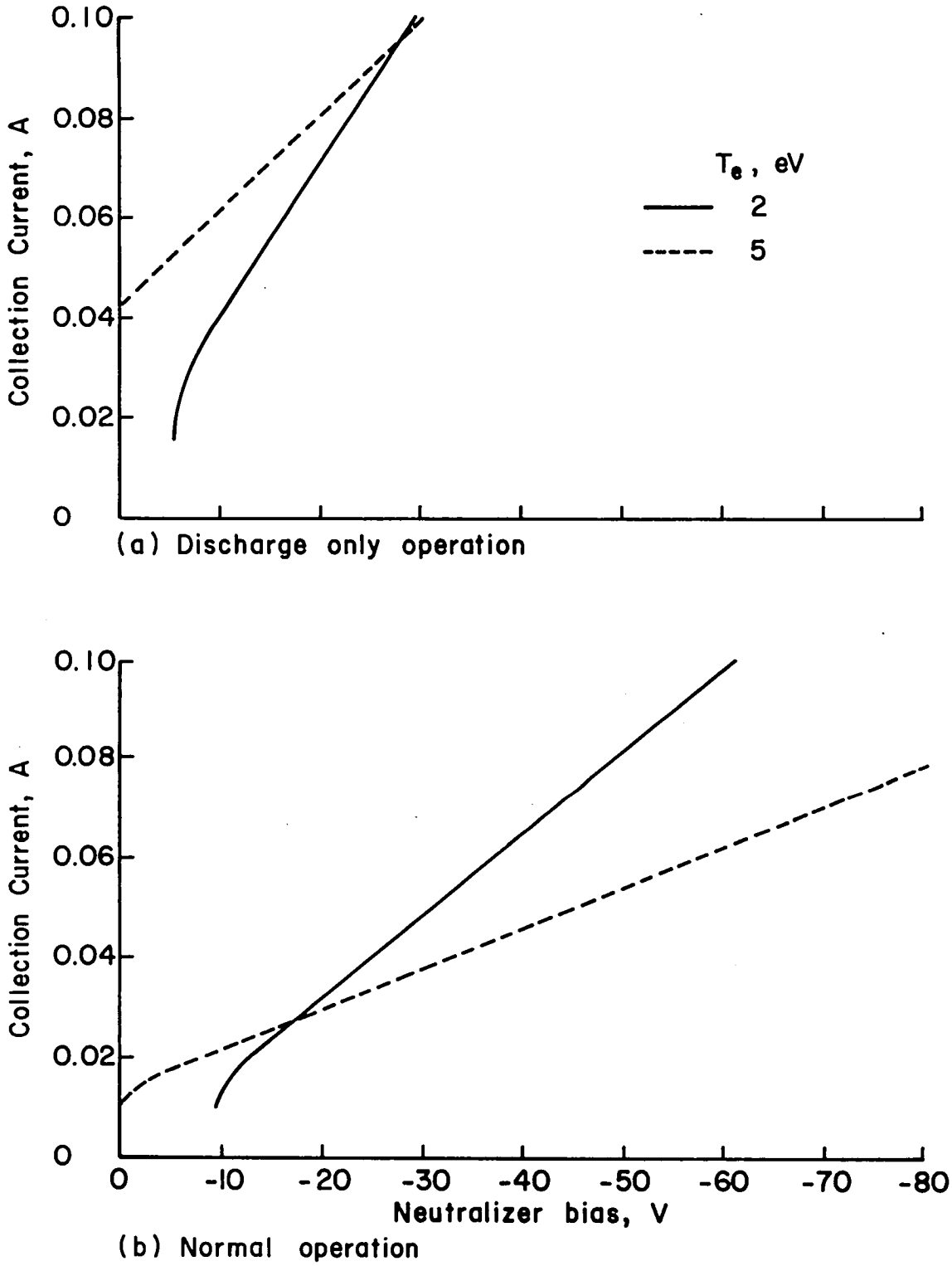


Fig. 10 - Theoretical ground-screen collection current as a function of negative neutralizer bias.

neutralizer plume and the charge-exchange density given earlier, this potential difference was 7-20 V for normal operation and 9-26 V for discharge only operation. In going from the ion beam density to the less dense charge-exchange plasma, a negative difference is obtained from Eq. (A-7). This density produced difference is therefore subtracted from the sum of the other two differences to give the value shown in Fig. 10.

### Charge-Exchange Ion Current to Accelerator

The case of most interest is the one in which the negative accelerator grid of a nonoperating thruster collects ions from the charge-exchange plasma of the other thruster, which is operating in the discharge only mode. Using the reference location for far field calculations that is described in Appendix B, the radius R is about 1.2 m and the angle $\theta$ about 115 degrees.

The plasma density at the nonoperating accelerator grid for these conditions was estimated at about 7-12 $\times$ $10^{10}$ $m^{-3}$ (2-5 eV). Using the Bohm current density (Eq. (A-3)) and the exposed accelerator grid area (corresponding to a radius of about 7 cm), a collection current of about 0.3 $\mu$A would be expected. An accelerator grid at -1500 V, however, will draw from a far larger area than just the exposed accelerator grid. Using a spherical space-charge-flow solution as a basis for estimation, the current collected from a large, uniform plasma of the density calculated above was found to be several $\mu$A. The sheath thickness for such a collection process, though, was found to be >3 m. In flight, then, the influence of the negative accelerator grid should extend into the much denser plasma that is found closer to the operating thruster. One should therefore expect a collection current higher than

several μA, but it does not appear practical to estimate how much higher.

## Current to Spacecraft

The methods of Appendix A were used to calculate the charge-exchange plasma density near the center of the downstream face of the spacecraft, midway between the two thrusters. The radius R was about 0.7 m at this location, while the angle θ to the beam direction was about 140 degrees. A thruster operating normally contributed about $6\text{-}4 \times 10^{10}$ $m^{-3}$ (2-5 eV), while one in the discharge only mode contributed $11\text{-}7 \times 10^{10}$ $m^{-3}$.

Even assuming electron arrival at the instability limit value of current density (Eq. (A-2)), the total for both thrusters operating would be only 0.02 $A/m^2$. Even though the spacecraft is quite large, it should be evident that the electron current that can be collected in this manner is quite limited.

Any insulated surface would, of course, assume a potential such that electron arrival would be reduced to that of the ions, a value about 1000 times smaller. Even conducting surfaces would seldom have potentials such that collection up to the instability limit would be observed.

## Plasma Potential at Survey Plane

An estimate of the plasma potential variation expected at the survey plane can be obtained from the sum of the potential difference due to electron conduction and the "barometric" effect. The difference due to conduction is the sum of the plume difference and the radial difference in the ion beam. It is 2.0 V for normal operation (2-5 eV)

and 0.7 V for discharge only operation. The barometric effect is, when corrected to the densities at the survey plane, 7-20 V for normal operation and 9-26 V for discharge only operation.

For an 85 mA neutralization current, the total difference from a magnetic field line that intercepts the neutralizer radius at the thruster to the beam axis, the total potential difference should be 9-22 V for normal operation and 10-27 V for discharge only operation. If the potential difference due to conduction is ignored for discharge only operation, because neutralization is due to discharge-chamber electrons, the latter is only $\sim$1 V lower. If absolute values are of interest, the charge-exchange plasma close to the neutralizer should be about 10 V positive relative to the neutralizer. The charge-exchange plasma density drops by about a factor of 3 in going from the vicinity of the neutralizer along a magnetic field line to the probe survey plane. The potential should therefore drop by about 2-5 V over the same distance, giving a positive charge-exchange plasma potential of about 8-5 V relative to the neutralizer.

## COMPARISON WITH FLIGHT DATA

The most important test of any analytical approach is its agreement with reality. In this analysis, reality is represented by the experimental SERT II flight data.

### Neutralizer Coupling

Operation of the two SERT II thrusters with one neutralizer grounded and the other biased positive permits a comparison of flight data with the neutralizer coupling characteristics of Figs. 7 and 8. These theoretical coupling characteristics have been replotted to show the shift in neutralization current between the two neutralizers for various positive biases in Fig. 11.

Also shown in Fig. 11 are the SERT II flight data. The operating condition for both theory and experiment was one thruster (No. 1) in the discharge only mode and the other thruster (No. 2) operating normally. As mentioned in the Problem Definition section, the discharge only thruster emitted sufficient discharge-chamber electrons to neutralize the associated ion beam. In fact, the average of the total neutralizer emission for SERT II data was only 72 mA. This was therefore the value used in the theoretical calculations.

The experimental data show a shift from all neutralizer 2 emission at a neutralizer 1 bias of 12-16 V to all neutralizer 1 emission at a neutralizer 2 positive bias of 6 V. Neither of the axially symmetric models show the required sensitivity to positive bias.

The plume penetration model, on the other hand, does show the required sensitivity. It is not clear, however, that the details of the curve shape are justified for this model. If the details of the

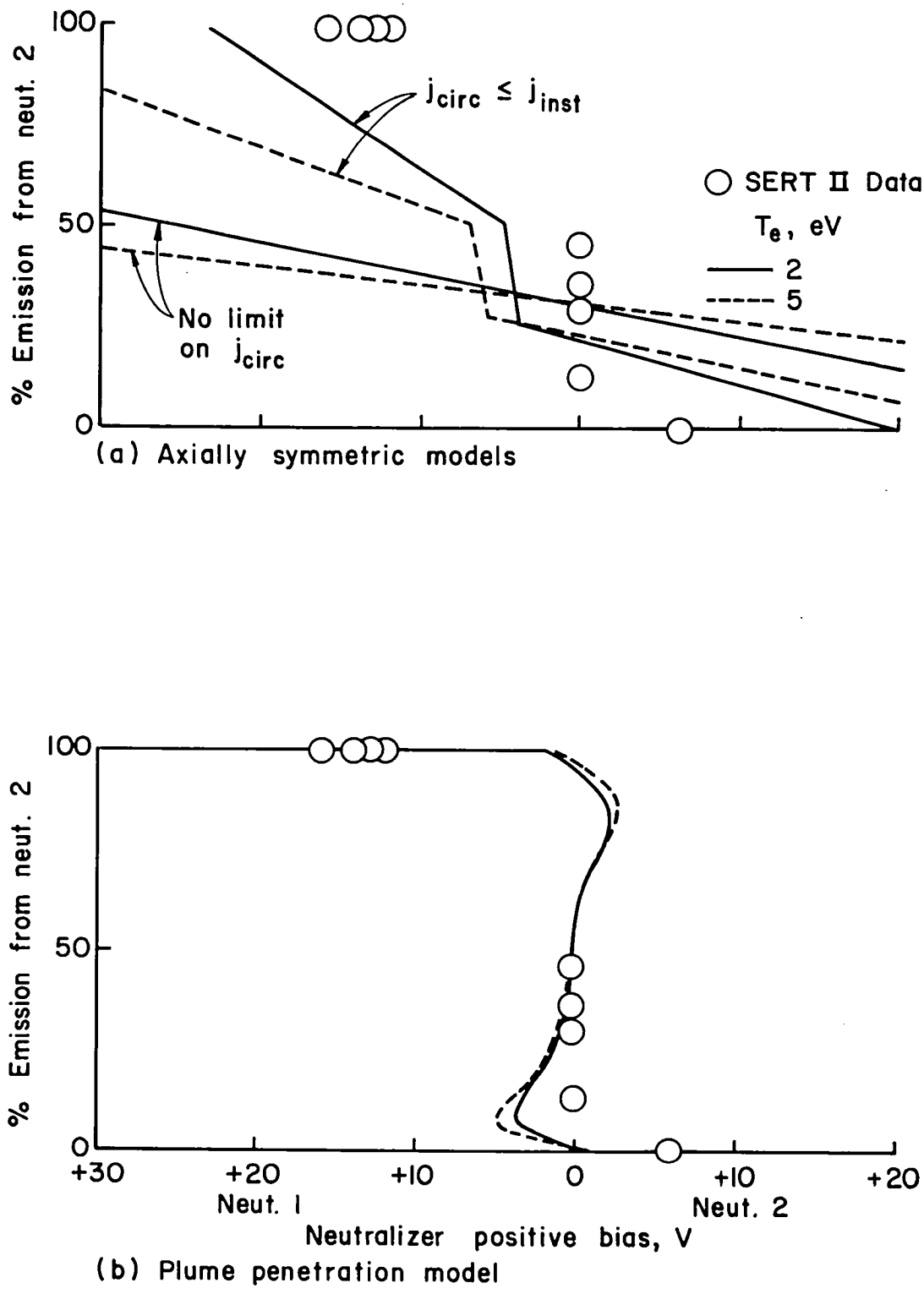


Fig. 11 - Distribution of emission currents between neutralizer for various positive biases.

curve shape are ignored, Fig. 8 clearly shows a generally lower potential for discharge only operation at the same current as normal operation. This lower impedance coupling of the discharge only thruster results from the higher plasma densities and shorter plume length in that mode. The experimental observations of relative coupling ease are thus theoretically supported.

The high experimental conductivity between the effluxes of the two thrusters appears justified by calculations for the overlap region fairly close to the spacecraft. An important factor in the calculated results was the use of opposite polarities for the two thrusters. This orientation also provided a magnetic barrier between the neutralizer electrons and the ambient space electrons having a temperature of $\sim$0.2 eV. Without this barrier, the low-energy space electrons might have replaced the higher energy electrons from the thrusters. The magnetic field configuration used was therefore probably responsible for the electron temperatures being close to those obtained in ground tests.

## Current to Ground Screen

The neutralizers of the SERT-II thrusters were operated negative of the spacecraft. For such operation, large excess neutralizer currents were observed. The analysis indicated that under these bias conditions substantial electron currents would be expected to go to the inner edge of the ground screen surrounding the ion beam. The comparison of theory and experiment is shown in Fig. 12 for the discharge only and normal operation modes. The experimental data are about 10-100 percent above the theoretical curves.

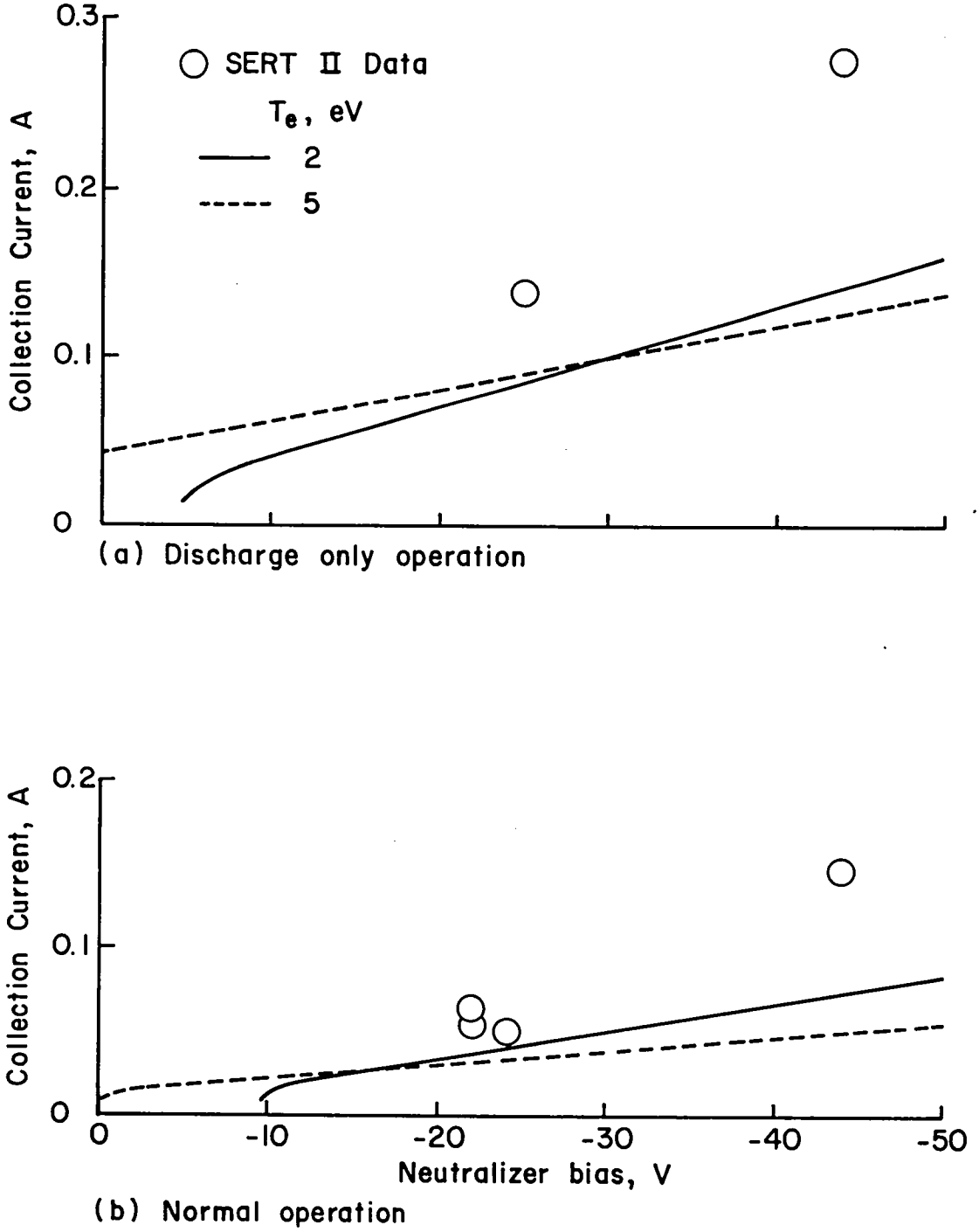


Fig. 12 - Excess neutralizer emission as a function of negative neutralizer bias.

This degree of agreement is reasonable, but a possible explanation can be given for the theoretical values being low. There was a portion of the ground screen located at a radius between the neutralizer and the ion beam. After operation, this part of the ground screen had a bright appearance, indicating some bombardment by plume ions. A high conductivity path from the plume to this location might therefore also be expected. The conductivity of such a path would depend on plume configuration details that were not available. Analysis was thus not practical. The direction of the error between theory and experiment in Fig. 12 suggests that such a conductive path existed.

The theory used for Fig. 12 indicates that a significant electron current to the ground screen may exist in the absence of a negative neutralizer bias (5 eV) electron temperature. Those portions of the emission curves, though, are close to the minimum currents assumed necessary for plume penetration. The plasma calculations are particularly questionable near a transition condition, so firm conclusions should not be drawn about the existance of a zero bias current to the ground screen from Fig. 12.

### Charge-Exchange Ion Current to Accelerator

One SERT II thruster was operated in the discharge only mode. At the same time, the other thruster was nonoperative. A -1500 V potential on the nonoperative accelerator resulted in a 0.1 mA ion current being collected. The nearest alternate current indications that would have been possible with the telemetry used were 0 and 0.2 mA. The 0.1 mA value thus has an accuracy of about ±100 percent. The theoretical value for the same conditions was found to be somewhere above several μA.

No firm conclusions should therefore be drawn concerning the magnitude of the collected ion current.

### Plasma Potential at Survey Plane

Surveys of plasma potential were obtained with an emissive probe during SERT II thruster operation. From Figs. 3 and 5, the magnetic field line connecting the neutralizer to the survey plane intercepted the survey plane about 18 cm from the beam axis.*

For zero bias operation, SERT II data showed potential differences between ion beam centerline and ±18 cm from this location of about 20-25 V for normal operation and 5-10 V for discharge only operation. These results indicate ∿5 eV electron temperature for normal operation and ∿2 eV for discharge only operation. The lower temperature for discharge only operation is consistent with electrons escaping from the discharge chamber and none actually needed from the neutralizer. The ∿5 eV electron temperature is also consistent with the absolute plasma potential ±18 cm from the centerline with normal operation. The measured value was ∿4 V while the 5 eV value was about 5 V.

The effect of neutralizer bias on experimental plasma potential is also available. With a positive neutralizer bias of +46 V the difference increases to ∿50 V, while with a negative neutralizer bias of ∿44 V the difference decreases to $\lesssim$20 V. It appears that the reduced difference for a negative bias is associated with the axially symmetric part of the ground screen current collection calculations. The higher difference for the positive bias appears more likely to result from a

---

*The probe did not pass through the azimuthal location of the neutralizer. But axial symmetry was assumed to obtain plasma potential at the survey plane.

higher electron injection energy, probably due to local electric field effects of nearby parts of the ground screen.

# CONCLUDING REMARKS

As indicated in the Introduction, plasma calculations should be considered of limited accuracy - often no better than agreement within a factor of two. The following comments should be interpreted in this accuracy context.

Axially symmetric models were found inadequate for neutralization electron conduction to the ion beam. A plume penetration model was developed for this conduction problem, and showed qualitative agreement with flight data. In the absence of data to the contrary, this plume penetration model is recommended for future neutralizer calculations. In the SERT II configuration, conduction of neutralization electrons between thrusters was experimentally demonstrated in space. The analysis of this configuration presented herein suggests that the relative orientation of the two magnetic fields was an important factor in the observed results. Specifically, the opposed field orientation appeared to provide a high conductivity channel between thrusters, and a barrier to the ambient low-energy electrons in space.

The SERT II neutralizer currents with negative neutralizer biases were up to about twice the theoretical predictions for electron collection by the ground screen. An explanation for the higher experimental values was a possible conductive path from the neutralizer plume to a nearby part of the ground screen.

Plasma probe measurements on SERT II gave the clearest indication of plasma electron temperature, with normal operation being near 5 eV and discharge only operation near 2 eV.

# APPENDIX A

## PLASMA CALCULATIONS

This appendix is not intended as a survey of plasma physics calculations. The intent, instead, is to cover those aspects of such calculations as are most important to the analysis presented herein. In particular, voltage-current relationships and limiting values of various electron currents are discussed.

The saturation current density of electrons, $j_{sat}$, is obtained when all the electrons in one directional hemisphere are collected by a surface. For this value of collection to actually take place, the surface should be at local plasma potential. The significance of the saturation current density is that it represents the approximate upper limit for electron collection by an electrode surface without the electrode becoming more positive than the plasma. Attempting to increase the electrode potential above that of the plasma may, depending on electron availability, simply increase the plasma potential. Although the sheath thickness is not a factor in the electron collection currents herein, the current collection at an electrode may also increase as it is made more positive than the plasma because the increasing sheath thickness results in collection from a larger effective area. This saturation current density is

$$j_{sat} = 2.68 \times 10^{-14} \, n \, T_e^{1/2}, \qquad \text{(A-1)}$$

where n is the plasma density (electrons or ions) and $T_e$ is the electron temperature.

For significant electric fields induced within the plasma, electron currents can exceed the value given above. If the electron currents are sufficiently large, they become limited by two-stream instability. Ignoring the small correction for a finite ion mass, two-stream instability is encountered above about 3.28 times the current density given above.[3]

$$j_{inst} = 8.79 \times 10^{-14} \; n \; T_e^{1/2} \qquad \text{(A-2)}$$

The approximate equivalent to saturation current density for ions is the current density due to Bohm velocity, or ion acoustic velocity. This current density is

$$j_B = 1.57 \times 10^{-15} \; n \; (T_e/M_i)^{1/2} \; , \qquad \text{(A-3)}$$

where $M_i$ is the ion mass in amu (200.6 for Hg). Bohm velocity applies to the self expansion of a plasma with low energy ions - at ion acoustic velocity. It does not apply to an energetic ion population, such as beam ions from a thruster.

For the voltage-current characteristics of the bulk plasma, consider first the case in which there is either no magnetic field or the electron current is parallel to the magnetic field. In this case the classical conductivity has been shown to be a good approximation. For the conditions of interest ($n = 10^{12}$-$10^{16}$ $m^{-3}$ and $T_e$ = 1-5 eV) this conductivity is approximately[4]

$$\sigma_o = 10^3 \; T_e^{3/2} \; . \qquad \text{(A-4)}$$

Coulomb collisions are assumed to dominate in this conductivity, which should be sufficiently accurate for the conditions of interest. Note that the plasma density does not appear in the preceding conductivity equation. A more exact equation would show a slowly varying logarithmic factor related to plasma density, reflecting the slight dependence of Coulomb cross section on this density. Ignoring this small effect, the change in charge carrier density with plasma density is balanced by the change in collision frequency for these charge carriers.

Although the conductivity is nearly independent of plasma density, the maximum permissible current density is a direct function of this density. Depending on the circumstances, Eq. (A-1) or Eq. (A-2) should be used. For an electrode that is not disturbing the plasma, Eq. (A-1) would be appropriate for maximum electron collection. For the bulk of a plasma, or for an electrode that is positive relative to the local plasma potential, Eq. (A-2) would be more appropriate.

These current limits should not be thought of as definite limits that will show up in an experimental current measurement. It was mentioned earlier that an electrode can be collecting the saturation value, then show an increase in current collection as the electrode is made more positive. In this case the increase in current may result from an increase in sheath thickness. A similar "elasticity" is associated with the two-stream instability limit. Assuming a current is at this instability limit and the driving electric field is increased, the experimental current density would still be expected to increase. This is because the increased electric field would increase the electron drift velocity above the instability limit, resulting in increased scattering of electrons, so that some of this increased drift velocity would be

transformed into random velocity. The increased electron temperature associated with this increased random velocity would, from Eq. (A-2), then permit an increased current density for the same plasma density. This interplay between plasma properties and process limits is something that must frequently be considered in plasma calculations.

Electron conduction across a magnetic field is also of interest, and is best described by the semiemperical Bohm diffusion value.[5,6] The current density across a magnetic field, using Bohm diffusion is given by[7]

$$j_m = e\ n\ \Delta V/16\Delta\int \bar{B} \times d\bar{\ell}\ , \qquad \text{(A-5)}$$

where e is the electronic charge, $\Delta V$ is the applied potential difference, and $\Delta\int \bar{B} \times d\bar{\ell}$ is the magnetic field integral across which $\Delta V$ is applied. The use of the integral $\Delta\int \bar{B} \times d\bar{\ell}$ in the conduction across a magnetic field is much more convenient than the detailed magnetic field distrubution.[7] Precise calculation of conduction across a magnetic field would require additional integration over the potential difference. With the other uncertainties associated with the calculations herein, though, the use of finite intervals was felt to be adequate. Making the numerical substitutions in Eq. (A-5), it becomes

$$j_m = 1.00 \times 10^{-20}\ n\ \Delta V/\Delta\int \bar{B} \times d\bar{\ell}\ . \qquad \text{(A-6)}$$

There are some important considerations in the use of Eqs. (A-5) and (A-6). Perhaps the most important is that of circulating or Hall currents. When an electron current is flowing radially inwards or

outwards across a magnetic field, circulating currents are also generated around the axis of symmetry. The existence of these circulating currents is essential for the relationship between $j_m$ and $\Delta V$ shown in Eq. (A-6). If some aspect of the geometry prevents these circulating currents from flowing, the potential difference required to produce a given current density will be greatly reduced from the value given above. The experimental sequence is that the applied electric field produces a transverse electron drift. If inhibited, this transverse drift produces another electric field normal to the applied one. This induced electric field results in a rapid electron drift to satisfy the original electric field. The solid-state Hall effect is an example of no circulating current being permitted.[8] The induced electric field in that case results in conduction in the original electric field direction being the same as if no magnetic field were present.

The magnitude of the circulating current density is also of interest. From a general derivation, the magnitude of the circulating current density is $\omega\tau$ times the radial current density, where $\omega$ is the cyclotron frequency and $\tau$ is the mean collision time.[8] For Bohm diffusion, turbulent "collisions" are such that the circulating current density (normal to the applied field) is about 16 times the current density in the direction of the applied field. (It is precisely 16 from the value of Bohm diffusion, but it should be recalled that this value only approximately describes experimental results.) If we start at some low value of applied electric field and slowly increase it, the circulating current density would increase linearly with the applied electric field. At a sufficiently large applied field, the drift velocity would reach some instability limit. In the absence of any more specific information,

this instability limit is assumed to be the same as that obtained in the absence of a magnetic field, Eq. (A-2). It may be of interest that the drift velocity associated with Eq. (A-2) is close to the acoustic velocity for the electron gas, $(\gamma kT_e/m_e)^{1/2}$. One might therefore expect an instability limit near this drift velocity from fluid-dynamic considerations, with or without the involvement of a magnetic field.

Again, one should not expect this current limit to be clear-cut and definite. If the drift velocity associated with the circulating current density exceeds the instability limit, then rapid randomization would be expected to result in an increase in electron temperature. This increase would, in turn, permit an increase in permissible drift velocity. If the electron temperature is held nearly constant by some process, such as the rapid increase in excitation cross section above a certain electron energy, then one might expect other instabilities to develop. These other instabilities could serve to permit large increases in current density in the direction of the applied electric field.

Only the potential difference associated with electron currents have been discussed in this appendix. There are also potential differences associated with plasma density differences. In the absence of any relative drift velocity between electrons and ions, these latter potential differences are predicted by the "barometric equation,"

$$n = n_o \text{ Exp } (V/T_e) \ , \qquad \text{(A-7)}$$

with the plasma potential (V) defined as zero at a plasma density of $n_o$. For the analysis herein, the potential differences due to density

differences were added to the potential differences due to current flows. With the large uncertainties associated with various aspects of these calculations, this superposition assumption should not significantly degrade the accuracy of the results.

The barometic equation has a theoretical limit that is seldom considered. If the ion beam, for example, is allowed to expand indefinitely, then the continual decrease in ion density should result in a continuously decreasing potential and a continuous ion acceleration. Conservation of energy would not permit such a continuous increase in ion energy. Assuming a low enough density of the background space plasma, the electron temperature in the ion beam should eventually decrease as the beam expands. In practice, the mean free path of ion-beam electrons is large enough that the thermal conduction of the electrons in the downstream direction must also be included in any energy balance. Over the beam lengths investigated in ground tests, this thermal conduction in the downstream direction has obscured any electron cooling due to ion-beam expansion. The magnetic field configuration external to the SERT II thrusters is believed effective in isolating the region near the thrusters from the more distant space plasma. No significant cooling effect due to beam expansion is therefore expected in the SERT II space tests, and has not been considered in the analysis presented herein.

# APPENDIX B

## CHARGE-EXCHANGE PLASMA

For the charge-exchange density, the calculation method was based on studies presented previously.[9,10] The equation used was

$$n = [J_b^2(1-\eta_u)/r_b R^2 \eta_u]\ P\ , \qquad \text{(B-1)}$$

where $J_b$ is the beam current, $\eta_u$ is the propellant utilization, $r_b$ is beam radius, R is the radius of interest from a reference point slightly downstream of the thruster (one thruster radius for far-field calculations), and the parameter P is:

| θ, deg | P | θ, deg | P |
|---|---|---|---|
| 0-90 | $2.5 \times 10^{12}$ | 140 | $3.2 \times 10^{11}$ |
| 100 | $1.8 \times 10^{12}$ | 150 | $1.9 \times 10^{11}$ |
| 110 | $1.2 \times 10^{12}$ | 160 | $1.1 \times 10^{11}$ |
| 120 | $8.2 \times 10^{11}$ | 170 | $6.7 \times 10^{10}$ |
| 130 | $5.1 \times 10^{11}$ | 180 | $3.8 \times 10^{10}$ |

The angle θ is measured from the beam direction. For close field measurements, flow considerations indicate that a reference point location one beam radius downstream of the thruster would be a better choice. The experimental data agreed within about a factor of two with this correlation, except for $\theta < 90$ degrees, where higher experimental densities were also possible.

Some corrections were required for this basic calculation method. The mean electron temperature within the charge-exchange plasma was 2.5-3.5 eV for the experimental data base, while the electron temperature in the ion beam was about twice that. No temperature correction was used in calculations for an electron temperature of 5 eV. For a 2 eV temperature, the density was increased by a factor of $2.5^{1/2}$.

A correction was also used for the effect of ion energy on charge-exchange ion energy. For 1000 eV (the data base energy), the Hg charge-exchange cross section is about $6 \times 10^{-19}$ $m^2$. For the 3000 eV SERT II energy, the cross section would be about $5 \times 10^{-19}$ $m^2$, while for the 40 eV energy it would be about $9 \times 10^{-19}$ $m^2$. The calculated densities were corrected by the ratio of the appropriate charge-exchange cross section to $6 \times 10^{-19}$ $m^2$.

All other parameters required for the analysis used the calculated densities and the equations presented in Appendix A. Note that the beam radius, $r_b$, in this appendix has to do with the escape of neutrals, and is thus about 7 cm, regardless of the ion beam profile.

# APPENDIX C

## NEUTRALIZER PLUME

The current to the ion beam through the neutralizer plume is a clear departure from axial symmetry. A method of calculation is presented in this appendix for the plume region, based on Bohm diffusion and a physical understanding of plasma processes.

The nonsymmetrical addition of a current to a plasma can often be approximated with a symmetrical configuration. This is because nonsymmetrical configurations tend to evolve into symmetrical ones. In Fig. 13, a neutralizer current is introduced so that it must travel through considerable charge-exchange plasma to reach the ion beam. Due to the magnetic field, the neutralizer current would tend to have a large circumferential component, as also indicated in Fig. 13. This tendency to spread out and distribute a neutralizer current would result in much of the current conduction through the charge-exchange plasma approximating axial symmetry.

The problem of interest for the SERT II thruster, and most plasma-bridge neutralizers, is when and how to treat departures from axial symmetry. We know that the neutralizer plume can provide a conductive path through which most of the neutralizing current can flow. Also, the plume width when this occurs is roughly equal to the plume length. The configuration of most interest for non-symmetric conduction, then, is a short, dense plasma column extending from the neutralizer tip to the ion beam, through the less dense charge-exchange plasma. This configuration is indicated in a somewhat idealized manner in Fig. 14. The conduction of the neutralizing current density in the neutralizer plume

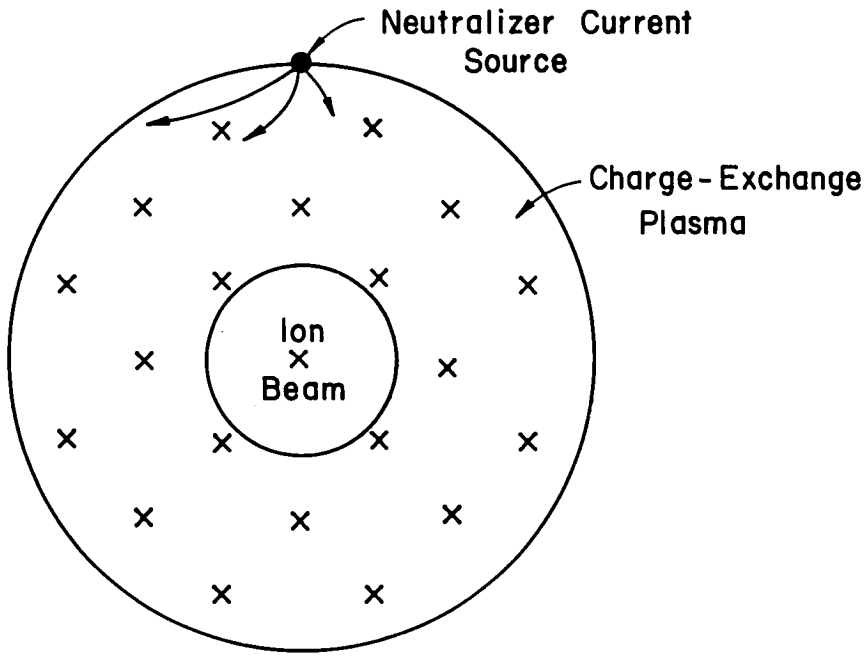


Fig. 13 - Conduction from neutralizer that approximates axial symmetry.

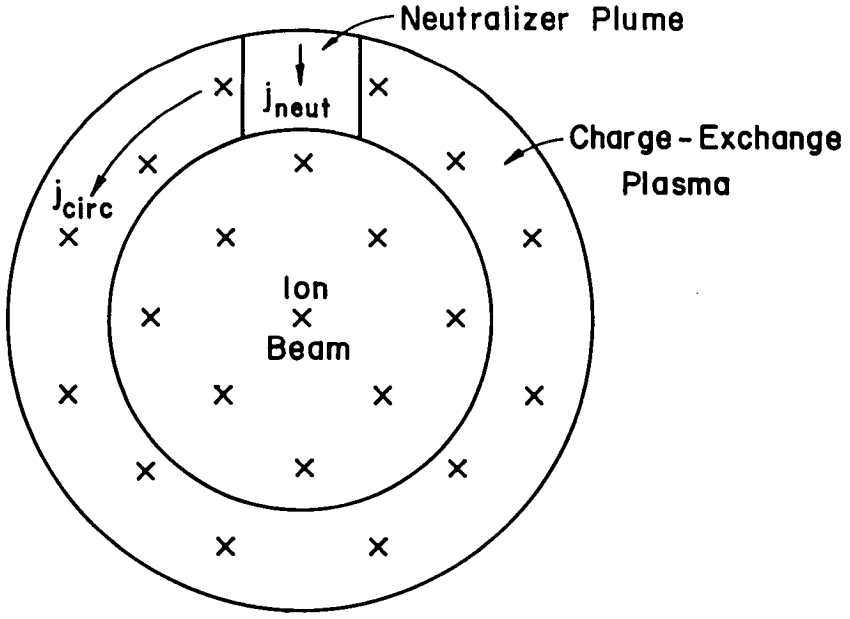


Fig. 14 - Conduction from neutralizer that departs significantly from axial symmetry.

will tend to produce some circulating current density in the charge-exchange plasma, as also indicated in Fig. 13. The bulk of any induced current in the charge-exchange plasma, though, will probably be localized near the plume.

If the charge-exchange plasma can sustain a circulating current density of the required magnitude for Bohm diffusion (16 $j_{neut}$), then the voltage drop in the neutralizer plume should be adequately described by Eqs. (A-5) and (A-6). The vector diagram for current density within the neutralizer plume is indicated in Fig. 15(a) for this condition.

If, however, the required circulation current cannot be sustained, then an induced electric field, $E_{ind}$, will be produced in the plume plasma, as indicated in Fig. 15(b). This induced field is in the circumferential direction and produces a component of drift velocity in the direction of the neutralizer current density, $j_{neut}$.

The basic assumption made for plume conduction is that the diffusion processes for the two cases (Figs. 15(a) and (b)) are identical, except for the rotation of total electric field and total current density. A minor assumption is also made that the 3.6 degree angle between E and $j_{tot}$ in Fig. 15(a) can be ignored. This last assumption is the reason for $E_{tot}$ being shown as normal to $j_{tot}$ in Fig. 15(b). With these two assumptions, the potential difference over the plume length can be calculated.

Consider first the total electric field. To conform with previous equations, a total potential difference will be calculated first. Bohm diffusion is associated with a current of approximately $j_{tot}/16$. From Eq. (A-5), the voltage difference for this current density is

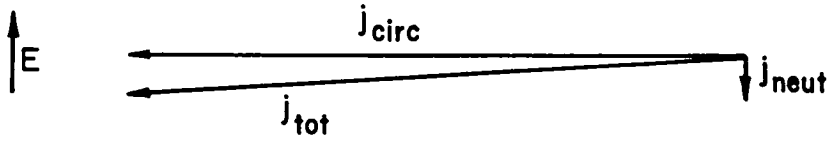


(a) Normal Bohm Diffusion

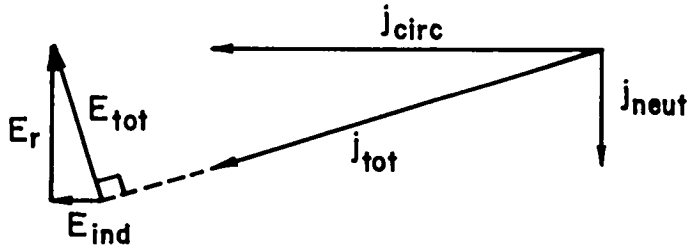


(b) Diffusion with Limited Circulation Current Density

Fig. 15 - Diffusion in neutralizer plume. The magnetic field is assumed to be directed into the paper. The radius from the beam axis increases toward the top of the page.

$$\Delta V_{tot} = j_{tot} \Delta \int \bar{B} \times d\bar{\ell}/e\, n \ . \qquad \text{(C-1)}$$

The radial component of this voltage is of interest. From the geometrical relationships of Fig. 15(b),

$$\Delta V_r = \Delta V_{tot} \, (j_{circ}/j_{tot}) \ . \qquad \text{(C-2)}$$

With Eq. (C-1) substituted in Eq. (C-2),

$$\Delta V_r = j_{circ} \Delta \int \bar{B} \times d\bar{\ell}/e\, n \ . \qquad \text{(C-3)}$$

The plasma properties in the plume must still be evaluated for Eq. (C-3). It does not appear realistic to use plume conditions observed in the absence of a significant magnetic field, such as in a neutralizer component test. The same radial potential difference that draws electrons into the ion beam will reflect low-energy plume ions, thereby reducing the plume density from the no magnetic field case. A reasonable and simple choice for plume density is a value just sufficient to carry the required total current density. With this choice, the plume density is

$$n_p = n_{ce} \, (T_{e,ce}/T_{e,p})^{1/2} (1 + j_{neut}^{\ 2}/j_{circ}^{\ 2})^{1/2} \ . \qquad \text{(C-4)}$$

Substitution of Eq. (C-4) into Eq. (C-3) yields

$$\Delta V_r = j_{circ} (T_{e,p}/T_{e,ce})^{1/2} \Delta \int \bar{B} \times d\bar{\ell}/e\, n_{ce} (1 + j_{neut}^{\ 2}/j_{circ}^{\ 2})^{1/2} . \qquad \text{(C-5)}$$

For the case where $j_{neut}/j_{circ}$ is small, the circulation current should result in a rapid mixing of plume and charge-exchange electrons and a rapid approach to axial symmetry. For a small $j_{neut}/j_{circ}$, with $j_{inst}$ (Eq. (A-2)) used for $j_{circ}$,

$$\Delta V_r = 5.49 \times 10^5 \, T_e^{1/2} \Delta \int \bar{B} \times d\bar{\ell} \, . \qquad \text{(C-6)}$$

This solution is the same as axially symmetric conduction through the charge-exchange plasma, with $j_{circ}$ equal to $j_{inst}$ in the charge-exchange plasma. Another condition of interest is one with a large value of $j_{neut}/j_{inst}$. For this condition, with $j_{circ}$ again equal to $j_{inst}$ in the charge-exchange plasma,

$$\Delta V_r = 5.49 \times 10^5 \, T_{e,p}^{1/2} \Delta \int \bar{B} \times d\bar{\ell} (j_{circ}/j_{neut}) \qquad \text{(C-7a)}$$

or

$$\Delta V_r = 4.82 \times 10^{-8} \, (T_{e,p}/T_{e,ce})^{1/2} \Delta \int \bar{B} \times d\bar{\ell}/j_{neut} \, . \qquad \text{(C-7b)}$$

For a large value of $j_{neut}/j_{circ}$, there should be little mixing of plume and charge-exchange electrons.

For low neutralizer currents, the conduction has been shown to approximate radial symmetry with conduction through the charge-exchange plasma alone. For large neutralizer currents, the conduction is approximated by Eqs. (C-7). For the latter conditions, there should be little mixing of plume and charge-exchange electrons, due both to the relatively small transverse electron velocity and the higher plume density. Also, the bulk of the conduction should be through the plume.

The transition between low and high neutralizer currents involves conditions that are difficult to calculate. Decreasing from high neutralizer currents, Eqs. (C-7) can be assumed to apply up to a maximum $\Delta V_r$ equal to that given by Eq. (C-6). Increasing from low neutralizer currents, axially symmetric conduction (Eq. (A-6)) through the charge-exchange plasma can be assumed to apply up to the same maximum $\Delta V_r$. If there were a current range between these two approaches, the $\Delta V_r$ could be assumed constant at the maximum value. For the cases of interest in the analysis presented herein, there is an overlap for the two approaches. Each approach is assumed valid up to the $\Delta V_r$ for which there is a common solution. In general, whether or not there is an overlap for the two approaches depends to a large extent on the relative conduction areas for neutralizer plume and charge-exchange plasmas.

The transition condition for the analysis herein can be obtained by equating potential differences from Eqs. (A-6) and (C-7b). Expressing the result in terms of currents and conduction areas, instead of current densities,

$$J_{n,trans} = 2.20 \times 10^{-14} \, n_{ce} (A_{ce} A_p T_{e,p}^{1/2} T_{e,ce}^{1/2})^{1/2} \quad . \quad (C-8)$$

The area $A_p$ is the conduction area of the plume at the radius of interest, while the area $A_{ce}$ is the alternate conduction area through the axially symmetric charge-exchange plasma.

## REFERENCES


1. W. R. Kerslake and S. Domitz, "Neutralization Tests on the SERT II Spacecraft," AIAA Paper No. 79-2064, Oct./Nov. 1979.

2. W. R. Kerslake, Private Communication, Feb. 1980.

3. O. Buneman, "Dissipation of Currents in Ionized Media," Phys. Rev., Vol. 115, pp. 503-517, Aug. 1959.

4. L. Spitzer, Jr., Physics of Fully Ionized Gases, Interscience Publ., New York, 1956, pp. 73-86.

5. D. Bohm, "Qualitative Description of the Arc Plasma in a Magnetic Field," in The Characteristics of Electrical Discharges in Magnetic Fields," (A. Guthrie and R. K. Wakerling, eds.), McGraw-Hill Book Co., New York, 1949, pp. 1-12.

6. F. F. Chen, Introduction to Plasma Physics, Plenum Press, New York, 1974, p. 169.

7. H. R. Kaufman and R. S. Robinson, "Plasma Processes in Inert Gas Thrusters," AIAA Paper No. 79-2055, Oct./Nov. 1979.

8. C. Kittel, Introduction to Solid State Physics, John Wiley and Sons, New York, 3rd ed. (1966), pp. 240-244.

9. H. R. Kaufman, "Charge-Exchange Plasma Generated by an Ion Thruster," NASA Contr. Rep. CR-135318, Dec. 1977.

10. H. R. Kaufman and M. R. Carruth, Jr., "Charge-Exchange Plasma Environment for an Ion Drive Spacecraft," JPL Publ. No. 79-90, Oct. 1979.